Tissue Eng Regen Med (2022) 19(5):1089–1098
https://doi.org/10.1007/s13770-022-00451-7

Online ISSN 2212-5469 TERM

ORIGINAL ARTICLE

Decellularized Human Adipose Tissue as an Alternative Graft Material for Bone Regeneration

Woo Beom Ahn[1] · Yu Bin Lee[2] · Yi-Hwa Ji[3] · Kyoung-Sik Moon[2] · Hyon-Seok Jang[3] · Sun-Woong Kang[4,5]

Received: 19 February 2022 / Revised: 4 March 2022 / Accepted: 7 March 2022 / Published online: 12 May 2022

Abstract

BACKGROUND: Tissue engineering approaches to treat damaged bone include various tissue transplants such as autologous, allogeneic, and xenografts. Artificial materials have been widely introduced to meet the demand for graft materials, but insufficiency in supply is still not resolved. In this study, human adipose tissue, easily obtained from the human body, was harvested, and the tissue was decellularized to fabricate a decellularized human adipose tissue matrix (DM) as an alternative graft material.

METHODS: Human adipose tissue was obtained via liposuction. The obtained fresh adipose tissue sample was cut into pieces then put into decellularization solution (1% antibiotic–antimycotic solution and 1% phenylmethanesulphonyl fluoride). Lipids were further removed via treatment in isopropanol. The sample was then subjected to another enzymatic digestion and lipid removal processes. The obtained decellularized adipose tissue matrix was lyophilized to form a graft material in disc shape.

RESULTS: Decellularization was confirmed by nuclear staining methods and detection of RNA and DNA via PCR. Bone morphogenetic protein 2 (BMP2)-loaded DM showed the ability to form new bone tissue when implanted in subcutaneous tissue. In recovery of a mouse calvarial defect model, BMP2-loaded DM exhibited similar levels of bone tissue regeneration efficiency compared with a well-defined commercial product, BMP2-loaded CollaCote®.

CONCLUSION: The DM developed in this study is expected to address the problem of insufficient supply of graft materials and contribute to the treatment of bone defects of critical size as an alternative bone graft material with preserved extracellular matrix components.

Keywords Bone tissue engineering · Decellularization · Human adipose tissue · Critical sized bone defect · Bone graft material

Woo Beom Ahn and Yu Bin Lee have contributed equally to this study as the first authors.

Hyon-Seok Jang and Sun-Woong Kang have contributed equally to this study as the corresponding authors.

✉ Hyon-Seok Jang
omfs1109@korea.ac.kr

✉ Sun-Woong Kang
swkang@kitox.re.kr

[1] Department of Medicine, Graduate School of Medicine, Korea University, Seoul 02841, Republic of Korea

[2] Department of Advanced Toxicology Research, Korea Institute of Toxicology, Daejeon 34114, Republic of Korea

[3] Department of Dentistry, Korea University Ansan Hospital, Ansan 15355, Republic of Korea

[4] Research Group for Biomimetic Advanced Technology, Korea Institute of Toxicology, Daejoen 34114, Republic of Korea

1 Introduction

The supply of materials is a very important issue in tissue engineering approaches for the treatment of bone tissue damage [1]. Autologous and allografts have been used because of their relative immunological safety and therapeutic efficacy by maintaining bone tissue components [2]. However, there is a clear limitation in supply, and so the use of xenografts is also being considered at the expense of immune side effects [3]. Engineered biomaterials, which can be easily manufactured and supplied, are also offing effective treatments. Advances in biology have made compositional analysis of the bone tissue extracellular matrix (ECM) possible, and engineered biomaterials have been constructed from selected materials with a focus on the known components of the ECM [4]. A scaffold using synthetic or natural polymers is being developed as a functionalized bone graft material by mimicking the ECM and presenting biological signals such as bone morphogenetic protein 2 (BMP2) [5–7]. In other words, biomaterials that consider not only the well-defined biochemical properties of intrinsic ECM, but also mechanical properties such as porosity and stiffness, have come to function as a method to repair damaged bone tissue within a predictable range with few adverse effects.

However, existing artificial biomaterials have not yet fully mimicked the biological functions of natural ECM [4]. Although multiple components are being combined to form well-defined biomaterials that sufficiently mimic the functions of the ECM, ideal materials are still under investigation. Therefore, decellularized ECM matrices that remove cells to preserve native tissue ECM components to avoid immune responses on transplantation are receiving significant attention [8]. In addition, methods are being prepared to address the shortage of supply, a limitation of existing tissue transplantation, by decellularizing other living tissues other than bone tissue. Fat will be a very powerful resource in this regard. The ECM of adipose tissue is composed of molecules such as collagen, fibronectin, and laminin that aid in cell adhesion and migration [9]. The ECM of bone tissue also contains high proportions of collagen types I, III, and V [10]. Collagen enhances cellular function by acting as a depot for biological factors such as BMP2 through charge–charge interactions [11]. In addition, adipokines rich in ECM components are known to promote angiogenesis that helps bone tissue regeneration [12]. Adipose tissue is removed during a variety of surgical procedures and is readily obtained from autologous tissue. Therefore, adipose tissue–derived decellularized matrix may be a good choice for obtaining a matrix that mimics the components and functions of bone tissue ECM.

In this study, we investigated whether the matrix formed by decellularization of adipose tissue can act as a material for bone tissue regeneration. Decellularization was performed using human adipose tissue with sodium dodecyl sulfate (SDS) treatment (Fig. 1). Decellularized matrices were prepared via freeze-drying and standardized protocols for commercialization. The success of decellularization was confirmed by detecting the nucleus, residual DNA, and RNA; the bone tissue regeneration ability was confirmed by transplanting the BMP2-loaded substrate into the subcutaneous tissue of mice. In addition, we monitored the bone regeneration efficiency by transplanting the decellularized human adipose tissue matrix (DM) loaded with BMP2 onto a mouse calvarial defect model assuming critical-sized bone defect situations.

2 Materials and methods

2.1 Materials

All chemicals for the decellularization were purchased from Sigma Aldrich (St. Louis, MO, USA). BMP2 was purchased from R&D Systems (Minneapolis, MN, USA). CollaCote® was obtained from Integra Lifesciences Corporation (Princeton, NJ, USA).

2.2 Preparation of decellularized adipose tissue material for bone tissue regeneration

Human subcutaneous adipose tissue was obtained via selective liposuction from informed and consenting patients. The fresh adipose tissue sample was cut into pieces of 20–25 g. Four pieces of the adipose tissues were put into 100 mL of decellularization solution supplemented with 1% antibiotic–antimycotic solution (ABAM) and 1% phenylmethanesulphonyl fluoride (PMSF). The tissues were agitated for 5 days at 37 °C and 120 RPM (Shaking Incubator, FINEPCR, Gunpo, Korea). After agitation, three cycles of free-thaw in freezing buffer [hypotonic tris buffer (pH 8.0) containing 10 mM Tris base and 5 mM ethylenediaminetetraacetic acid (EDTA)] was conducted on the sample. The sample was then digested in enzymatic digestion solution #1 (0.25% trypsin, 0.1% EDTA) overnight. Lipids within the sample were removed via treatment in 99.9% isopropanol for 48 h. The sample was sequentially washed with a rinsing buffer [8 g/L NaCl, 200 mg/L KCl, 1 g/L Na_2HPO_4, and 200 mg/L KH_2PO_4 (pH 8.0)] for 30 min. The washed sample was again

[5] Human and Environmental Toxicology Program, University of Science and Technology, Daejeon 34114, Republic of Korea

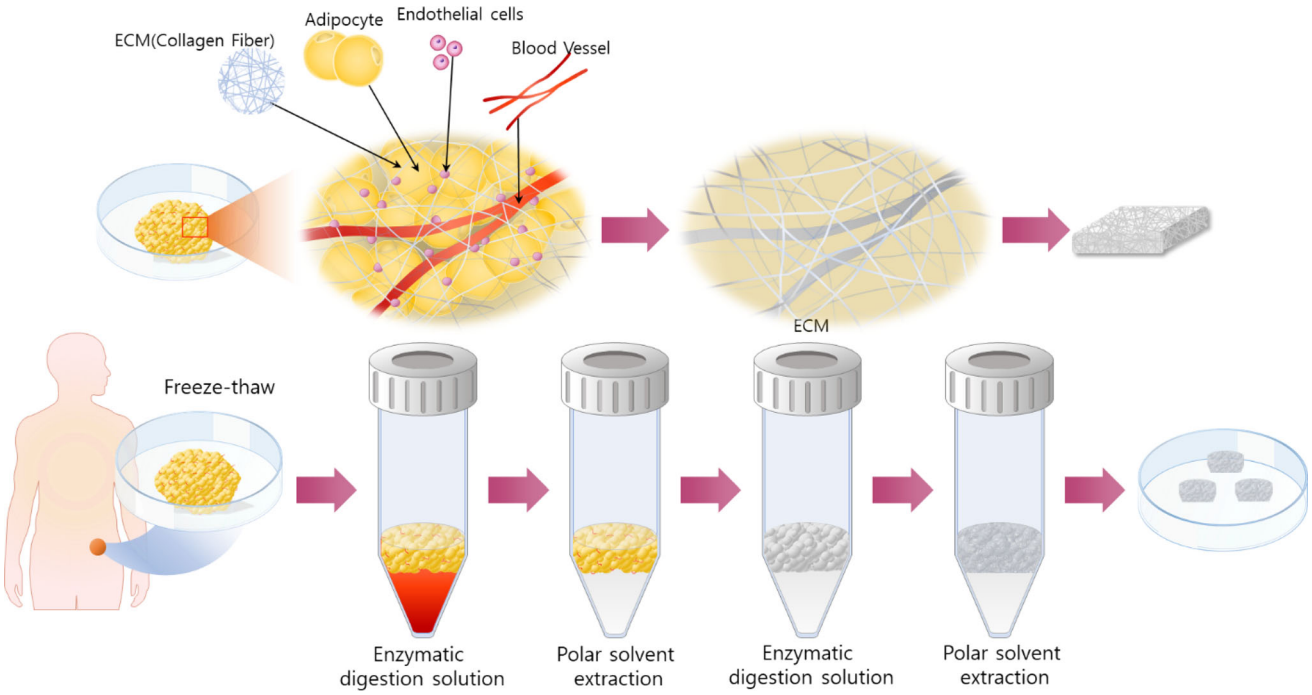

Fig. 1 Schematic diagram of the fabrication of the decellularized human adipose tissue matrix

subjected to the enzymatic digestion solution for 6 h. After a 30 min washing step in the rinsing solution, secondary enzymatic digestion was conducted with enzymatic digestion solution #2 [55 mM Na_2HPO_4, 17 mM KH_2PO_4, 4.9 mM $MgSO_4{\cdot}H_2O$, 15,000 U DNase Type II (from bovine pancreas), 12.5 mg RNase Type III A (from bovine pancreas), and 2000 Units Lipase Type VI-S (from porcine pancreas)] overnight. The sample was washed for 30 min, then treated with 99.9% isopropanol for 8 h. Then, 30 min washing in the washing solution and another 30 min washing in 70% EtOH were conducted. The obtained decellularized adipose tissue matrix was preserved in sterile phosphate buffered saline (PBS) supplemented with 1% ABAM at 4 °C until further use. Finally, 1 mg of DM was lyophilized to form a graft material in disc shape (diameter = 8 mm, thickness = 3 mm).

2.3 Examination of decellularization

Samples of native fat tissue and decellularized fat tissue were fix by 4% paraformaldehyde and then laid on glass slides. The samples were mounted using Vectashield mounting medium (H-1500, Vector Laboratories, Burlingame, CA, USA) containing 1.5 μg/mL 4′,6-diamidino-2-phenylindole (DAPI) to visualize nuclei. The stained slides were observed via fluorescence microscopy (Nikon ECLIPSE Ni, Nikon Corporation, Tokyo, Japan).

The presence of residual cells on the decellularized tissues was examined via electrophoresis. Purifications of RNA and DNA were conducted on samples of native fat tissue and decellularized fat tissue using TRIzol reagent (Life Technologies Corporation, Carlsbad, CA, USA) and DNAzol reagent (Gibco BRL, Grand Island, NY, USA), respectively. Samples were loaded on 1% agar gel and then, electrophoresis was conducted under 50 V (Mupid-21, Optima Inc. Tokyo, Japan).

2.4 Implantation of samples on mouse subcutaneous tissue and a mouse calvarial defect model

We used 5-week-old female Institute of Cancer Research (ICR) mice for the implantation of the samples on subcutaneous tissue; 8-week-old male Sprague Dawley (SD) rats were used for the calvarial defect model. Mice and rats were anesthetized via injection of ketamine (80 mg/kg body weight) and rompun (5 mg/kg body weight). Surgery sites were shaved and sterilized with 70% EtOH.

For implantation on subcutaneous tissues, two incisions (10 mm) were generated on the dorsal region. We then cut the underlying tissue to generate space for sample implantation. Two grafts (group 1: CollaCote® + 5 ug BMP2, group 2: Acellular matrix + 5 ug BMP2) were transplanted to the left and right incisions, respectively (N = 5). After implantation, the incision was sutured with silk suture.

For generation of the calvarial defect model, incision from the middle site of the eyes to the nuchal region was conducted to expose the cranium. A bone defect was then

generated on the skull via an 8 mm diameter surgical trephine bur (Marathon 3 Champion, Foshan Core Deep Medical Apparatus Co., Ltd., Foshan City, Guangdong, China). The samples of interest were prepared in a disc shape (diameter = 8 mm) prior to implantation. The defect was covered by the prepared sample (N = 5) and suture was conducted to close the surgery site.

2.5 Radiological and histological analysis

The new bone formation effect of the decellularized adipose tissue matrix was evaluated by implanting the developed graft materials on the mouse subcutaneous tissue and calvaria defect models. After 4 weeks, the mice were sacrificed via CO_2 gas. Tissues with implanted samples were immediately put into PBS solution.

Tissue samples extracted from the subcutaneous model were fixed with 10% neutral formalin. Then, the samples were observed via the SkyScan 1176 CT system (Bruker microCT, Kontich, Belgium). The X-ray source was set at 70 kV and 141 mA for shooting with the aid of a 0.5-mm thick aluminum filter.

The fixed samples of the subcutaneous model study were given to a pathological laboratory service (Korea CFC, Yongin, Korea) for hematoxylin and eosin (H&E) and Masson's trichrome (MT) staining. The stained slides were observed via a slide scanner (Panoramic scan II, 3D HISTECH Ltd, Budapest, Hungary).

The obtained skull tissues with the implanted grafts were washed with PBS then fixed with 10% neutral formalin. The tissue samples were analyzed using the SkyScan 1176 CT system with the same X-ray source conditions described above. For microcomputed tomography (microCT) analysis, three-dimensional (3D) images were produced using a CT reconstruction program (NRecon, Bruker microCT). The 360° rotational angle of specimens was set at 0.5° and 590 ms of exposure time. The bone volume (BV) per tissue volume (TV) was obtained using a reconstructed image analysis program (CTAn, data viewer, Bruker microCT) and the regenerative bone volume/bone volume (%) was calculated.

2.6 Statistical analysis

All quantitative data were presented as mean ± standard deviation (SD). Statistical significance was determined via one-way analysis of variance and Tukey's honestly significant difference tests ($p < 0.05$).

3 Results

3.1 Decellularization of human adipose tissue for bone tissue graft material

In this study, decellularized human adipose tissue matrix (DM) was fabricated with a standardized protocol (Table 1 and Fig. 1). The obtained adipose tissue showed a mixture of yellow and red coloring (Fig. 2A). In contrast, the decellularized tissue was opaque white. The decellularized tissue appeared to be clumped with fibrils. The change in color was due to the washing step, and the fibrous form was induced by collagen and other components of the adipose tissue ECM. Decellularization was demonstrated by detecting DNA and RNA signals in polymerase chain reaction (PCR) (Fig. 2B). Clearly observable bands of DNA and RNA appeared on the fresh human adipose tissue group indicating the existence of cells within the tissue. However, it was difficult to observe bands of DNA and RNA from the DM group. DAPI staining in this study also conducted to confirm the removal of cells from the adipose tissue via the decellularization process (Fig. 2C). On the fresh adipose tissue, a large number of nuclei signals stained with DAPI were found in adipose tissue. The structure of the fresh human adipose tissue could not be confirmed in the DIC image because it was difficult to transmit light owing to various substances including blood and fat. The DM group did not present notable nuclei signal, implying successfully conducted decellularization. It was observed that ECM in the form of fibers, such as collagen, appeared to be agglomerated in the DIC image.

Table 1 Summary of the decellularization process

Day	Process
1	Remove blood components via distilled water (DW) wash
	3 cycles of freeze–thaw
	Enzymatic digestion (digestion solution #1, overnight)
2, 3	Remove lipid via polar solvent (99.9% isopropanol)
4	Rinse (rinsing buffer, 3 times, 30 min each)
	Enzymatic digestion (digestion solution #1, 6 h)
	Rinse (rinsing buffer, 3 times, 30 min each)
	Enzymatic digestion (digestion solution #2, overnight)
5	Rinse (rinsing buffer, 3 times, 30 min each)
	Remove lipid via polar solvent (99.9% isopropanol)
	Rinse (rinsing buffer, 3 times, 30 min each)

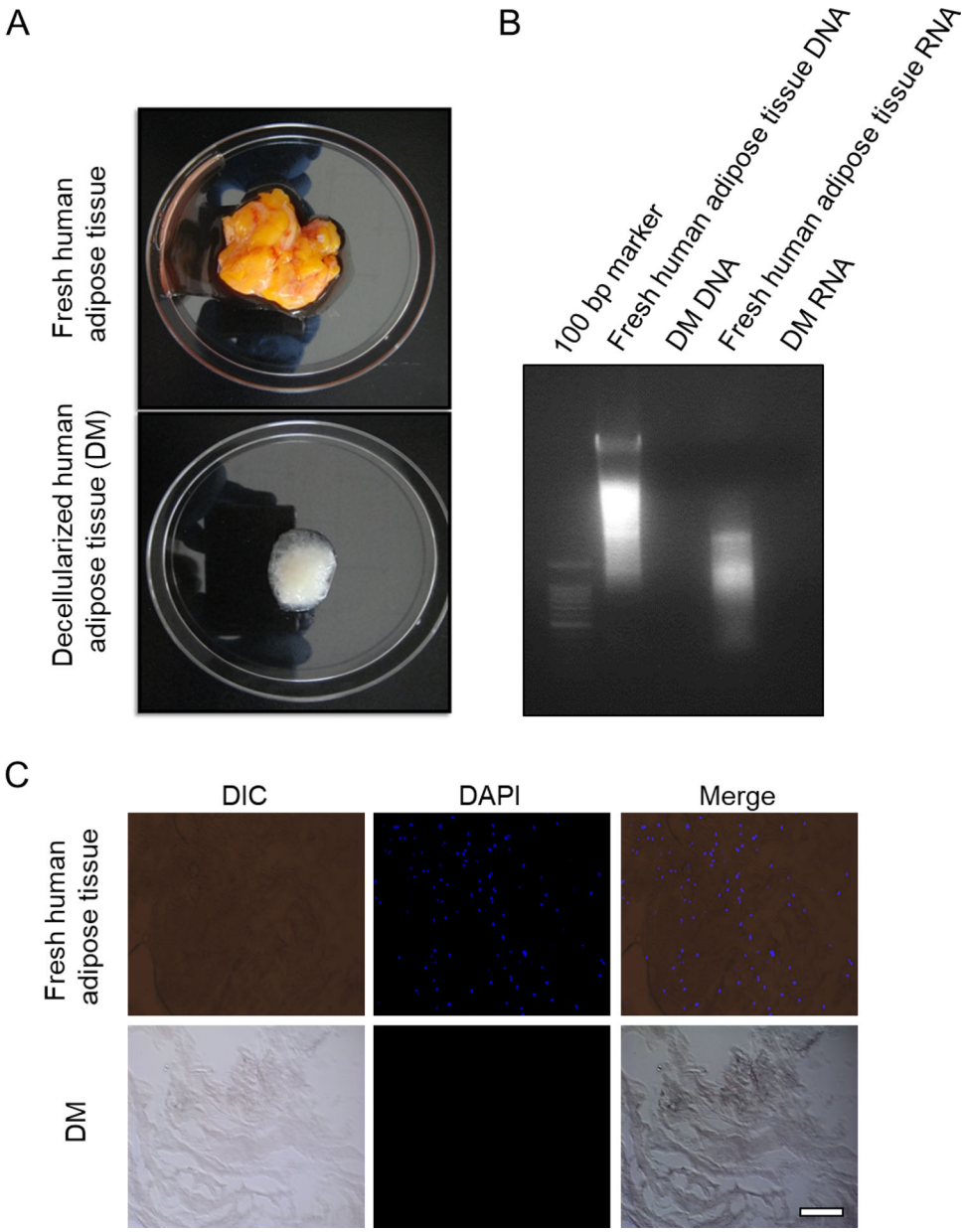

Fig. 2 Decellularization of the human adipose tissue matrix (DM). **A** Optical images before and after the decellularization of human adipose tissue. **B** Detection of DNA and RNA via polymerase chain reaction (PCR) analysis of fresh human adipose tissue and DM. **C** Images of 1.5 μg/mL 4′,6-diamidino-2-phenylindole (DAPI) staining of fresh human adipose tissue and DM (scale bar = 100 μm)

3.2 Structural observation of the DM

The microscopic structure of the fresh adipose tissue and DM was investigated via histological analysis (Fig. 3A). Both H&E and MT staining of the fresh human adipose tissue showed nuclei in the middle of the mesh-like structure (black arrows) presumed as ECM. However, none of the staining images of DM showed nuclei, but they did show tangled linear fibers assumed to be preserved ECM. Although the original mesh-like structure of ECM is changed during the decellularization process, stained ECM components (shown as blue on the MT staining of the DM) demonstrated ECM preservation after decellularization. The morphologies of the DM and CollaCote®, a commercial graft material, were then compared via scanning electron microscope (SEM) imaging (Fig. 3B). The CollaCote® had smaller pores that were homogeneously distributed along the whole construct as compared with those of DM. DM showed relatively larger pores generated by entangled thick fibrous structures.

3.3 New bone tissue formation on the graft materials after mouse subcutaneous implantation

We then loaded BMP2 onto both the DM and CollaCote®, and the materials were implanted on the subcutaneous region of mice to assess the ability of new bone tissue

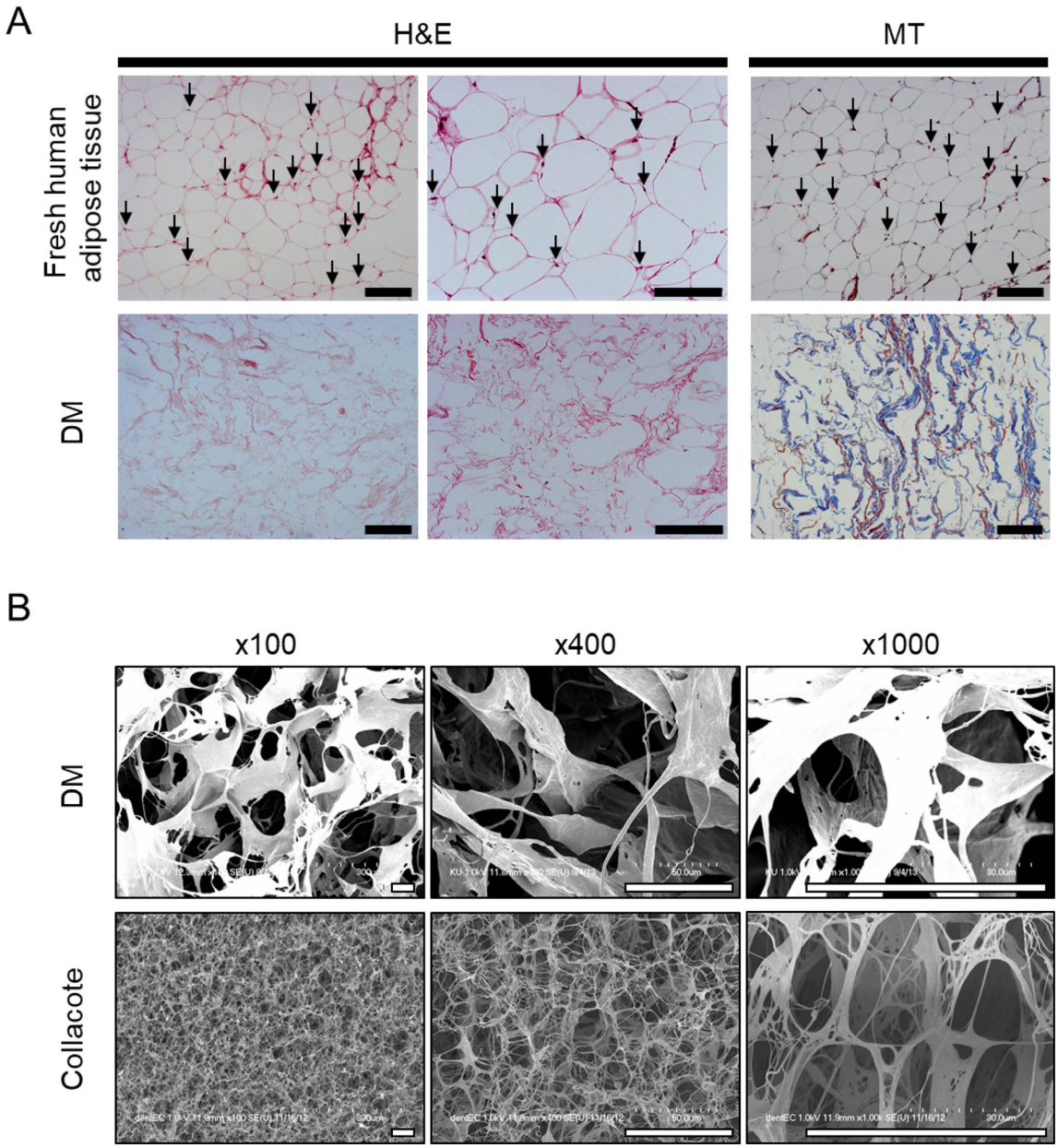

Fig. 3 Microscopic observation of human adipose tissue matrix (DM). **A** Images of hematoxylin and eosin (H&E) staining and Masson's trichrome (MT) staining (scale bar = 500 μm). The black arrows indicated nuclei within the fresh human adipose tissue. **B** Scanning electron microscope (SEM) images of DM and CollaCote® (scale bar = 500 μm)

formation (Fig. 4A). At week 4, samples of the BMP2-loaded DM showed relatively more recognizable white than that of the CollaCote® groups (Fig. 4B). In particular, the center of the acellular matrix presented more vivid white signal, indicating new bone tissue formation. The samples were analyzed via H&E and MT staining (Fig. 4C, D). White and light pink signals indicating bone tissue and matrix were distributed throughout the whole area of the DM, while in the CollaCote® group these signals were only present in the central area. Other area of the CollaCote® group, including the periphery, dominantly showed a deep red signal indicative of connective tissue. MT staining images of the DM also showed blue across the whole slide section, demonstrating bone tissue formation. However, the CollaCote® group only presented blue at center, with dark red connective tissue across most of the area. Magnified images of the DM group presented more densely formed bone tissues than those of the CollaCote® group.

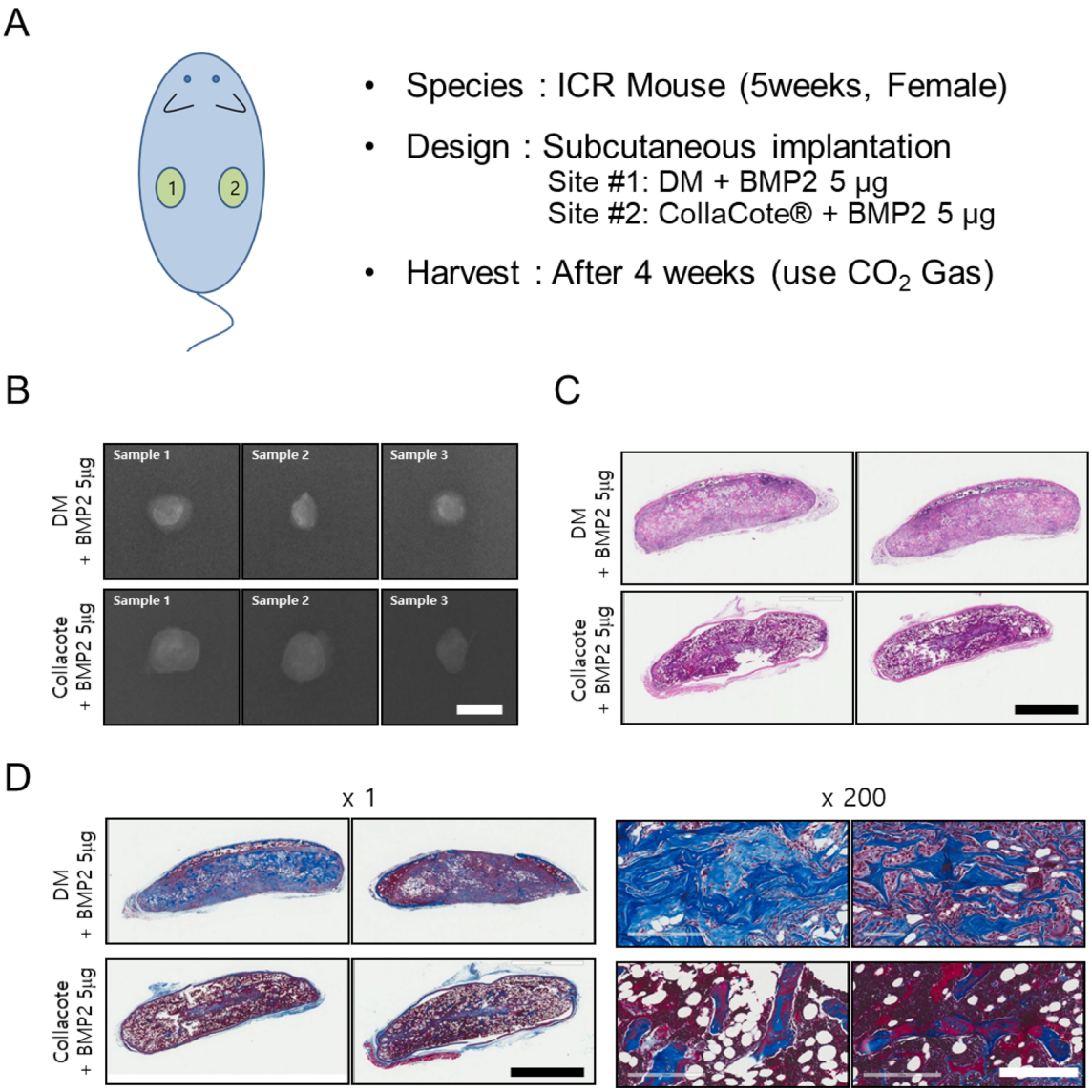

Fig. 4 Evaluation of new bone formation ability of the grafts on a mouse subcutaneous implantation model. **A** Schematic diagram of subcutaneous implantation of bone morphogenetic protein 2 (BMP2)-loaded human adipose tissue matrix (DM) and CollaCote®. **B** Soft X-ray images of BMP2-loaded grafts after 4 weeks of implantation on subcutaneous tissue (scale bar = 1 mm). Images of **C** hematoxylin and eosin (H&E) staining (scale bar = 2 mm) and **D** Masson's trichrome (MT) staining [scale bar = 2 mm (× 1), 200 μm (× 200)] of the BMP2-loaded grafts after 4 weeks of implantation on subcutaneous tissue

3.4 Treatment of critical bone defect by implantation of the grafts on a mouse calvarial defect model

The materials were then implanted in a calvarial defect model to assess the treatment capability of critical sized bone defects (Fig. 5A). Soft X-ray images of the BMP2-loaded DM group presented clearly distinguishable white objects at the circular defect sites. In addition, the white objects seemed to cover almost half of the defect area (Fig. 5B). The BMP2-loaded CollaCote® group also showed white objects covering almost half of the defect area. However, the implanted DM without BMP2 presented tiny fractions of white signals on the defect area. The CollaCote®-only group showed a very weak white signal compared with the groups loaded with BMP2. From comparison between the CollaCote®-only group and the DM-only group, it was found that the CollaCote®-only group showed a relatively clearer white signal and the coverage area was also wider. This trend was also observed in the microCT images (Fig. 5C). Both groups containing BMP2 showed newly formed bone tissues that densely filled more than half of the defect area. The CollaCote®-only group also showed improved bone tissue formation compared with the DM-only group, but the overall density of the newly formed bone tissue was lower than the BMP2-

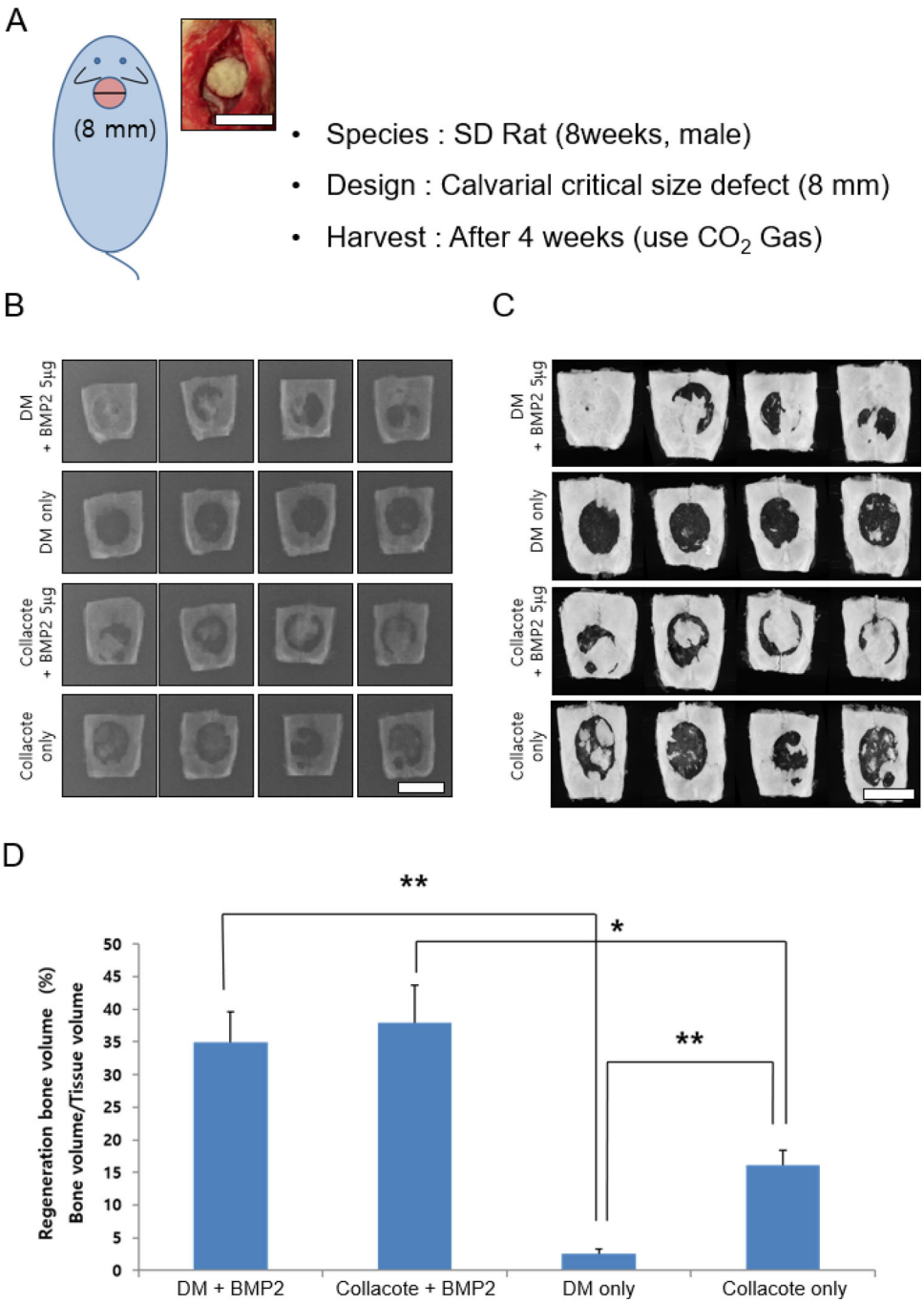

Fig. 5 Treatment of a critical sized calvarial defect model by implantation of the grafts. **A** Schematic diagram of implantation of the grafts (scale bar = 10 mm). Images of **B** soft X-ray (scale bar = 10 mm) and **C** microcomputed tomography (microCT) of the grafts after 4 weeks of implantation (scale bar = 10 mm). **D** Quantified regeneration bone tissue volume based on image analysis of microCT images. "*" and "**" indicated statistical significances (p value of < 0.05 and 0.02, respectively)

loaded groups, and some of the densely formed tissues were also fragmented. Quantitative analysis (Fig. 5D) of the BMP2-loaded groups exhibited recovery volume of $>$ 35%, suggesting that the dominant effect was owing to BMP2 rather than to the matrix materials themselves. The CollaCote®-only group showed $\sim$ 15%, while the DM-only group showed the lowest volume recovery ($< 5\%$), which may reflect structural differences, as shown in Fig. 3A.

4 Discussion

Decellularized adipose tissue is a resource that can be obtained through various routes such as liposuction, abdominoplasty, and breast reduction, and has been attracting attention as a material for tissue engineering for the past decade [13]. Similar to the ECM of bone tissue, decellularized adipose tissue also contains collagen (I, III, IV, V, VI) [14]. It has also been known to contain laminin, elastin, fibronectin, which induces cell adhesion, or

vascular endothelial growth factor (VEGF), which promotes cell activity, and fibroblast growth factor (FGF). DM can be manufactured in a variety of sizes and shapes to accommodate different defect sizes through freeze-drying and molding.

Figure 2 confirm the efficient removal of cells from the human adipose tissues via the standardized protocol. In a previous study of decellularized human adipose tissue, decellularization was demonstrated via DAPI staining that did not present a nuclei signal [15]. Adipose tissue has been decellularized through conventional methods of freeze/thaw, mechanical disruption, alcohol/solvent treatment, exposure to acid/base, and rinse [16]. After the lyophilization, the disc-shaped DM grafts showed physical properties that were easy to handle with tweezers, similar to other graft materials such as CollaCote®. The DM presented spatial support at the implanted sites (subcutaneous and calvaria regions) for more than 4 weeks.

The decellularization process in this study was performed similarly to that of conventional methods, and the results on Fig. 3 implied preserved ECM components, which are beneficial for bone tissue regeneration. Both materials are expected to allow cell adhesion and migration from surrounding tissue mediated by the pores, promoting new bone tissue formation on the materials [15]. We also assumed that the DM would lead to better bone tissue generation via promoted angiogenesis attributed to preserved ECM components and adipokines [17].

The interaction between a graft material and the surrounding tissue is a very important factor in bone tissue regeneration. On Fig. 4, CollaCote® presented cell migration from the surrounding tissue into the center was mediated by cell adhesive moieties of collagen and micro pores. Similarly, the DM promotes cell migration into the graft via preserved ECM components and pores. The preserved ECM components of DM may cause enhancement of cellular function for bone tissue regeneration that cannot be achieved with collagen alone. For example, adipokine is known to promote angiogenesis as adipose tissue-derived ECM [18]. Angiogenesis is closely related to bone formation, and biomolecules that induce angiogenesis such as VEGF have also been introduced in the field of bone tissue engineering [19]. We anticipated that the migration and activation of bone-forming cells may have been promoted by yet unproven ECM molecules preserved in DM. Angiogenesis is closely related to bone formation, and biomolecules that induce angiogenesis such as VEGF have also been introduced in the field of bone tissue engineering [19]. We anticipated that the migration and activation of bone-forming cells may have been promoted by yet unproven ECM molecules preserved in DM.

The treatment of the mouse calvarial defect model (Fig. 5) demonstrated that DM itself is not sufficient for bone tissue regeneration, but when BMP2 is loaded, it exhibits a therapeutic effect similar to that of a commercial product. BMP2 is a bioactive molecule that is very effective in bone tissue regeneration [20]. Numerous studies have observed that the delivery of BMP2 dramatically enhances the effect of bone tissue regeneration for both sustained and burst delivery [20–22]. On the basis of Figs. 3 and 4, it is difficult to achieve improved bone tissue regeneration with the DM itself compared to that with the CollaCote®. However, the enhanced effect when BMP2 was loaded suggests a synergistic relationship between the preserved ECM of the DM and BMP2 [23, 24]. As shown in Fig. 3B, we observed that the CollaCote® showed finer and more uniformly formed micropores than DM. In the subcutaneous model, the osteoinductive effect induced by BMP2 may have had a dominant effect on bone formation associated with the preserved ECM within the DM. However, in the calvarial defect model, the osteoconductive effect exerted from the surrounding bone tissue may also have influenced the new bone formation [25]. It is possible that DM and BMP2 loaded DM groups inhibited the penetration of bone forming cells from surrounding bone tissue compared to CollaCote and CollaCote + BMP2 groups. Although BMP2 loaded DM group showed high osteoinductivity, osteoconductivity was probably lower than that of BMP2 loaded CollaCote® group due to structural characteristics. In both the conventional models of subcutaneous implantation and in the calvarial defect models for verifying bone regeneration, the absence of an inflammatory response in the DM group suggests that DM is a graft material that minimizes the immune response of the decellularized matrix. However, additional investigations such as staining of immune cell markers may be necessary to clearly identify inflammation.

In conclusion, the DM is expected to address the problem of insufficient supply of existing bone regeneration graft materials. In addition, since it maintains ECM components, it has an advantageous synergistic effect with BMP2 and interacts with surrounding tissues for better treatment of bone defects. In conclusion, the decellularized matrix using human adipose tissue reported in this study offers a potential alternative and effective bone tissue regeneration material that overcomes problems of insufficient supply and immune side effects.

Acknowledgements This research was supported by the Korea Institute of Toxicology, Republic of Korea (1711133848 and 1711133843).

Declarations

Conflicts of interest There are no conflict to declare.

Ethical statement Human adipose tissue was obtained via liposuction in compliance with the guidelines of the Institutional Animal Care and Use Committee (IACUC) of Korea University Ansan Hospital (Approval Number: AS12194). All animal experiments were approved by the IACUC of Korea University (KUIACUC 2013-21). All animals were managed by following guidelines for the care and use of laboratory animals.

References

1. Amini AR, Laurencin CT, Nukavarapu SP. Bone tissue engineering: recent advances and challenges. Crit Rev Biomed Eng. 2012;40:363–408.
2. Baroli B. From natural bone grafts to tissue engineering therapeutics: brainstorming on pharmaceutical formulative requirements and challenges. J Pharm Sci. 2009;98:1317–75.
3. Drosse I, Volkmer E, Capanna R, De Biase P, Mutschler W, Schieker M. Tissue engineering for bone defect healing: an update on a multi-component approach. Injury. 2008;39:S9–20.
4. Aamodt JM, Grainger DW. Extracellular matrix-based biomaterial scaffolds and the host response. Biomaterials. 2016;86:68–82.
5. Dang M, Saunders L, Niu X, Fan Y, Ma PX. Biomimetic delivery of signals for bone tissue engineering. Bone Res. 2018;6:25.
6. La WG, Kang SW, Yang HS, Bhang SH, Lee SH, Park JH, et al. The efficacy of bone morphogenetic protein-2 depends on its mode of delivery. Artif Organs. 2010;34:1150–3.
7. Lee TJ, Kang SW, Bhang SH, Kang JM, Kim BS. Apatite-coated porous poly(lactic-co-glycolic acid) microspheres as an injectable bone substitute. J Biomater Sci Polym Ed. 2010;21:635–45.
8. Das P, Mishra R, Devi B, Rajesh K, Basak P, Roy M, et al. Decellularized xenogenic cartilage extracellular matrix (ECM) scaffolds for the reconstruction of osteochondral defects in rabbits. J Mater Chem B. 2021;9:4873–94.
9. Chun SY, Lim JO, Lee EH, Han MH, Ha YS, Lee JN, et al. Preparation and characterization of human adipose tissue-derived extracellular matrix, growth factors, and stem cells: a concise review. Tissue Eng Regen Med. 2019;16:385–93.
10. Lin X, Patil S, Gao YG, Qian A. The bone extracellular matrix in bone formation and regeneration. Front Pharmacol. 2020;11:757.
11. Migliorini E, Valat A, Picart C, Cavalcanti-Adam EA. Tuning cellular responses to BMP-2 with material surfaces. Cytokine Growth Factor Rev. 2016;27:43–54.
12. Ruiz-Ojeda FJ, Méndez-Gutiérrez A, Aguilera CM, Plaza-Díaz J. Extracellular matrix remodeling of adipose tissue in obesity and metabolic diseases. Int J Mol Sci. 2019;20:4888.
13. Flynn LE. The use of decellularized adipose tissue to provide an inductive microenvironment for the adipogenic differentiation of human adipose-derived stem cells. Biomaterials. 2010;31:4715–24.
14. Kim YS, Majid M, Melchiorri AJ, Mikos AG. Applications of decellularized extracellular matrix in bone and cartilage tissue engineering. Bioeng Transl Med. 2019;4:83–95.
15. Wang L, Johnson JA, Zhang Q, Beahm EK. Combining decellularized human adipose tissue extracellular matrix and adipose-derived stem cells for adipose tissue engineering. Acta Biomater. 2013;9:8921–31.
16. Keane TJ, Swinehart IT, Badylak SF. Methods of tissue decellularization used for preparation of biologic scaffolds and in vivo relevance. Methods. 2015;84:25–34.
17. Han SS, Choi JJ, Lee DE, Jang HS, Chung HM, Moon SH, et al. Histological analysis of in vitro co-culture and in vivo mice co-transplantation of stem cell-derived adipocyte and osteoblast. Tissue Eng Regen Med. 2016;13:227–34.
18. Panina YA, Yakimov AS, Komleva YK, Morgun AV, Lopatina OL, Malinovskaya NA, et al. Plasticity of adipose tissue-derived stem cells and regulation of angiogenesis. Front Physiol. 2018;9:1656.
19. Diomede F, Marconi GD, Fonticoli L, Pizzicanella J, Merciaro I, Bramanti P, et al. Functional relationship between osteogenesis and angiogenesis in tissue regeneration. Int J Mol Sci. 2020;21:3242.
20. Kang SW, Yang HS, Seo SW, Han DK, Kim BS. Apatite-coated poly(lactic-co-glycolic acid) microspheres as an injectable scaffold for bone tissue engineering. J Biomed Mater Res A. 2008;85:747–56.
21. Vantucci CE, Krishan L, Cheng A, Prather A, Roy K, Guldberg RE. BMP-2 delivery strategy modulates local bone regeneration and systemic immune responses to complex extremity trauma. Biomater Sci. 2021;9:1668–82.
22. Jung T, Lee JH, Park S, Kim YJ, Seo J, Shim HE, et al. Effect of BMP-2 delivery mode on osteogenic differentiation of stem cells. Stem Cells Int. 2017;2017:7859184.
23. Lee SS, Huang BJ, Kaltz SR, Sur S, Newcomb CJ, Stock SR, et al. Bone regeneration with low dose BMP-2 amplified by biomimetic supramolecular nanofibers within collagen scaffolds. Biomaterials. 2013;34:452–9.
24. Hong JY, Kang SW, Kim JW, Suh SW, Ko YJ, Park JH. Optimal condition of heparin-conjugated fibrin with bone morphogenetic protein-2 for spinal fusion in a rabbit model. Cytotherapy. 2014;16:1441–8.
25. Khan WS, Longo UG, Adesida A, Denaro V. Stem cell and tissue engineering applications in orthopaedics and musculoskeletal medicine. Stem Cells Int. 2012;2012:403170.